

EFFECT OF PRESSURE BROADENING ON THE RADIATIVE HEAT TRANSFER BY CO AND CH₄ GASES USING LINE-BY-LINE METHOD WITH LATEST HIGH TEMPERATURE DATABASE

by

**Yu YANG^a, Shu ZHENG^{a*}, Yuzhen HE^a,
Mingxin XU^a, Zixue LUO^b, and Qiang LU^{a*}**

^aNational Engineering Research Center of New Energy Power Generation,
North China Electric Power University, Beijing, China

^bState Key Laboratory of Coal Combustion,
Huazhong University of Science and Technology, Wuhan, Hubei, China

Original scientific paper
<https://doi.org/10.2298/TSCI210620319Y>

As the development of current propulsion technology such as gas turbine and rocket chamber moving to higher working pressure, the radiative parameters of fuel, such as CH₄ or CO, are required at elevated pressures, which in some cases are calculated without considering the pressure effect of line broadening. To investigate the pressure effect of line broadening on the radiative heat transfer, the radiative heat sources of a 1-D enclosure filled with CH₄/CO and Planck mean absorption coefficients at elevated pressures were calculated using the statistical narrow band and line-by-line methods. The radiative parameters were conducted using high temperature molecular spectroscopic (HITEMP) 2019 (for CO) and HITEMP 2020 (for CH₄) databases. The results showed that the pressure effect of line broadening on the calculations of radiative heat source of CH₄ can be ignored when HITEMP 2020 database was used. For CO medium, the pressure effect of line broadening was over 40% at 30 atmosphere in all cases whichever methods and databases were used. The pressure broadening has a strong effect on the Planck mean absorption coefficient below 1000 K for CH₄ and at the temperature of 500-900 K for CO at 30 atmosphere. The maximum pressure effects were 22% for CH₄ and 18% for CO at 30 atmosphere, which illustrated the pressure effect of line broadening needed to be taken into account in the calculation of Planck mean absorption coefficient.

Key words: gas radiation, Planck mean absorption coefficient, line broadening, HITEMP 2020 database, high pressure

Introduction

In real fire situations, the rate of fuel-burning depends on the radiative heat feedback from the flame to the fuel surface. For a 0.3 m diameter pool fire of CH₄, the ratio of radiative heat transfer to total heat transfer is around 55% and it increases with the pool diameter [1]. The radiative contribution of CO in combustion is always negligible since CO has a lower volume fraction, it is very different in gasification technology while syngas containing 30-40% CO [2]. In addition, CH₄ is the main component of natural gas, which is a clean fuel for power generation and can achieve zero-emission in combination with carbon capture and storage [3]. Therefore, substantial attention should be given to study the radiative heat transfer of CO and CH₄.

* Corresponding authors, e-mail: shuzheng@ncepu.edu.cn; qianglu@mail.ustc.edu.cn

In the past two decades, many methods have been developed to calculate radiative heat transfer of CO [2, 4] and CH₄ [5, 6] at atmospheric pressure. However, for the combustion in gasifiers [7] or gas turbine combustion chambers [8], the reaction pressure is much higher than atmospheric pressure. For example, the Bioliq gasifier [9] produced syngas from a biomass feedstock at a pressure of 40 atmosphere and an industrial gas turbine burner [10] with 5 MW output operated at a pressure of 15 atmosphere. Numerical simulations of such a gasifier or gas turbine require radiative parameters of participating medium at elevated pressures.

At present, many researchers have studied the gas radiation for elevated pressure [11, 12]. The absorption-line blackbody distribution function (ALBDF) and radiative heat transfer of H₂O and CO₂ in variable pressures had been calculated [13]. The results showed the ALBDF decreased with total pressure increased. The pressure affected the spectral line absorption coefficient by altering the line half-width (line broadening) and the increase of molecule density [14]. However, for the higher calculation efficiency, the pressure effect of line broadening was always ignored in the simulation at elevated pressures [15]. The absorption coefficient was simply considered to increase linearly with pressure [16].

Due to the complicated wavelength dependence of absorption coefficients, the Planck mean absorption coefficient was proposed and the corresponding radiative parameters were considered as wavelength independent [17]. Based on this assumption, the computation efficiency of radiative heat transfer can be dramatically improved. The Planck mean absorption coefficient was used as a gray-gas model [18] and had a good estimation on the radiation emission for the combustion system [19]. It was widely used in the prediction of radiative heat transfer of combustion systems in reduced pressures [20], atmosphere [19, 21] and elevated pressures [3, 22]. Nevertheless, the Planck mean absorption coefficient was considered to be independent of pressure [16], and the pressure effect of line broadening was neglected. The pressure effect of line broadening on the Planck mean absorption coefficient needs to be analysed, which is important to accurately predict radiative heat transfer in combustion at elevated pressures.

The novelty of this work is determining whether and when neglecting the pressure effect of line broadening would cause a strong impact on the radiative heat transfer. Firstly, the radiative parameters of CO and CH₄ at pressures of 1, 5, 10, and 30 atmosphere were generated using the line-by-line (LBL) and the statistical narrow band (SNB) methods based on the latest HITEMP databases which have been updated in 2019 and 2020 for CO and CH₄ [5], respectively. The radiative parameters were generally divided into two groups, one was generated considering the pressure effect of line broadening and the other one not. Subsequently, combined with two different groups of radiative parameters, the radiative heat sources at two different cases were calculated by the discrete-ordinate method (DOM) in a 1-D parallel plate model. The Planck mean absorption coefficients of CO and CH₄ were also obtained. Finally, the results calculated with two different groups of radiative parameters were compared and discussed.

Methodology

The LBL method

In the LBL method, the absorption coefficient of each band at wavenumber ν was given [23]:

$$\kappa_{\nu} = N \sum_i S_i(T) F_i(\nu) \quad (1)$$

where N is the molecule number density, S_i – line intensity of the i^{th} spectral line and F_i – Lorentz line shape profile and can be obtained:

$$F_i(\nu) = \frac{\gamma_i}{\pi \left[(\nu - \nu_{0i})^2 + \gamma_i^2 \right]} \quad (2)$$

where γ_i is the half-width of i^{th} spectral line and expressed:

$$\gamma_i = P\gamma_{i,\text{latm}} = P \left(\frac{T_0}{T} \right)^n \left[\gamma_{\text{air}} \left(1 - \frac{P_s}{P} \right) + \gamma_{\text{self}} \frac{P_s}{P} \right] \quad (3)$$

where $T_0 = 296$ K is the reference temperature, T , n , γ_{air} , γ_{self} , P , and P_s are the temperature of the medium, the coefficient of temperature dependence, the air-broadened half-width, the self-broadened half-width, the total pressure, and the medium partial pressure, respectively. If the pressure effect of line broadening was neglected, the eq. (3) can be transformed:

$$\gamma_i = \gamma_{i,\text{latm}} = \left(\frac{T_0}{T} \right)^n \left[\gamma_{\text{air}} \left(1 - \frac{P_s}{P} \right) + \gamma_{\text{self}} \frac{P_s}{P} \right] \quad (4)$$

The calculation of line intensity S_i can be found in [24].

For an absorbing, emitting medium, the radiative transfer equation (RTE) can be written:

$$\frac{\partial I_\nu}{\partial s} = -\kappa_\nu I_\nu + \kappa_\nu I_{b\nu} \quad (5)$$

The corresponding boundary conditions for a 1-D enclosure are written:

$$I_\nu(S_w, \Omega) = \varepsilon_{w,\nu} I_{b\nu,\nu} + \frac{1 - \varepsilon_{w,\nu}}{\pi} \int_{\bar{n}\Omega'} |\bar{n}\Omega'| I_\nu(S_w, \Omega') d\Omega', \text{ for } |\bar{n}\Omega'| > 0 \quad (6)$$

Once the radiative intensity is calculated by the DOM [25] with the absorption coefficient, the radiative heat flux can be obtained:

$$q(x_i) = \sum_{\text{all } \Delta\nu} \left(\sum_{n=1}^N \mu \bar{I}_{\nu,n,i} \omega_n \right) \Delta\nu \quad (7)$$

The radiative source term is then given:

$$-\frac{dq}{dx} = -\frac{q_{i+1} - q_i}{x_{i+1} - x_i} \quad (8)$$

The SNB method

The SNB method was conducted to calculate the average transmissivity of a narrow band [26]. For a medium with a path-length, L , a mole fraction, f , and a pressure, P , the average transmissivity of the SNB method was written [27]:

$$\bar{\tau}_\nu = \exp \left[-\frac{\pi B}{2} \left(\sqrt{1 + \frac{4SL}{\pi B}} - 1 \right) \right] \quad (9)$$

where

$$B = \frac{2\bar{\beta}_\nu}{\pi^2}, \quad S = \bar{k}_\nu f P, \quad \bar{\beta}_\nu = \frac{2\pi\bar{\gamma}_\nu}{\bar{\delta}_\nu}$$

where \bar{k}_ν , $\bar{\gamma}_\nu$, and $\bar{\delta}_\nu$ are the average coefficient absorption, the average half-width of spectral lines, and the average interval between spectral lines, respectively. The equations for calculat-

ing these parameters can be found in [28]. For a non-homogeneous and non-isothermal case, the Curtis-Godson approximation [29] was introduced to calculate the equivalent band parameters.

Once the average transmissivity of each discrete grid was obtained, the radiative intensity along a discrete direction, m , can be calculated by solving the RTE using the DOM. Finally, based on the radiative intensity in all directions, the radiative heat source at each grid point can be obtained [28].

The Planck mean absorption coefficient

The Planck mean absorption coefficient was a solution for gray-gas model and was established by [17]. It can be defined:

$$K_p = \frac{\int_0^{\infty} I_{b,v} \kappa_v dv}{\int_0^{\infty} I_{b,v} dv} = \frac{\pi}{\sigma T^4} \int_0^{\infty} I_{b,v} \kappa_v dv \quad (10)$$

where κ_v and $I_{b,v}$ are the spectral absorption coefficient and the spectral blackbody intensity at a wave number, v .

Validation of the SNB method

To validate the accuracy of the SNB method, the transmissivities calculated by the LBL method were introduced to serve as a benchmark. The HITEMP 2019 (for CO) and HITEMP 2020 (for CH₄) databases were adopted in the LBL and SNB methods. In the LBL method, the transmissivity at a wavenumber v over a path L was given:

$$\tau_{\text{LBL}} = \exp(-\kappa_v L) \quad (11)$$

The bandwidth of the LBL method was set as 0.02 cm⁻¹. For the purpose of comparing the transmissivity obtained by SNB method whose bandwidth was 25 cm⁻¹, the results of LBL method should be transferred to low resolution transmissivity:

$$\tau_{\text{LBL},\Delta v} = \frac{1}{\Delta v} \int_{v_0 - (\Delta v/2)}^{v_0 + (\Delta v/2)} \tau_{\text{LBL}} dv \quad (12)$$

where Δv is the bandwidth of the SNB method and v_0 – the central wavenumber of each band.

Figure 1 shows the transmissivities of CO and CH₄ calculated by the LBL and SNB methods. The maximum absolute errors of CH₄ and CO were -0.118 and 0.123, respectively. In general, the transmissivities calculated by LBL and SNB methods had an excellent agreement which demonstrated the high accuracy of the SNB method.

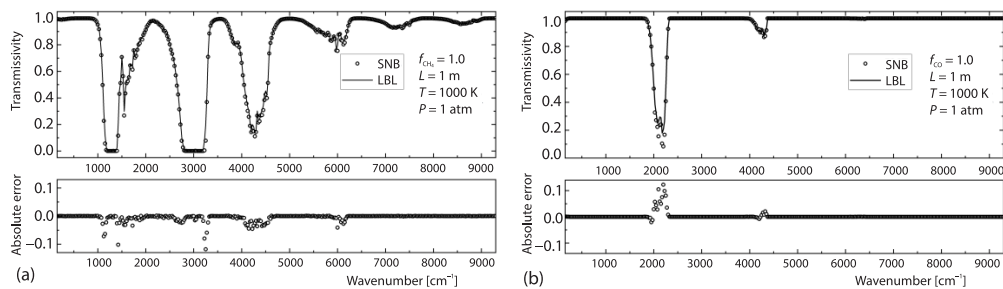


Figure 1. The transmissivities calculated by LBL and SNB methods and absolute errors for (a) CH₄ and (b) CO

Results and discussion

A 1-D parallel plate filled with CO or CH₄ gas was investigated in this study. The medium was bounded by black walls with a distance L equal to 1.0 m. The emissivities of both walls were 1.0. The bandwidth of LBL and SNB methods were chosen as 0.02 cm⁻¹ and 25 cm⁻¹ [30, 31]. The range of wavenumber was selected as 150-9300 cm⁻¹ since most spectral line located here both for CO and CH₄. The total pressures considered in this study were 1, 5, 10, and 30 atmosphere. To investigate the pressure effect of line broadening on the radiative heat transfer, the radiative parameters calculated using eqs. (3) and (4) at elevated pressures were both generated and compared. The DOM was used to solve the radiative heat transfer equation obtain the radiative heat sources for two different cases. The profiles of temperature and mole fraction of CO and CH₄ are similar to [12, 32] and were detailed in tab.1.

Table 1. The profiles of temperature and mole fractions of CO and CH₄

Case	Species	Temperature [K]	Mole fraction	Wall temperatures [K]	Pressures [atm]
1	CO/CH ₄	1000	1.0	300, 300	1, 5, 10, 30
2	CO/CH ₄	$400 + 1400\sin(\pi x/L)^2$	$\sin(\pi x/L)^2$	400, 400	1, 5, 10, 30

The Planck mean absorption coefficients at temperatures ranging from 300-1500 K with an interval of 100 K were obtained. The spectral absorption coefficient in eq. (6) was obtained from the radiative parameters calculated by the LBL method at total pressures of 1, 5, 10, and 30 atmosphere. The radiative parameters calculated using eqs. (3) and (4) were both generated to investigate the pressure effect of line broadening on the Planck mean absorption coefficient.

The legends $P\gamma$ and γ in figs. 2 and 3 represented the results calculated using eqs. (3) and (4), respectively. Since the radiative heat sources calculated using eqs. (3) and (4) were the same at 1 atmosphere, therefore, only a group of radiative heat sources at 1 atmosphere was plotted for each case. The pressure effect of line broadening on radiative heat source was described by:

$$\frac{|\nabla q_\gamma - \nabla q_{P\gamma}|}{(\nabla q_\gamma)_{\max}} \quad (13)$$

Radiative heat source for case1

An isothermal and homogenous CO and CH₄ were investigated in this case. As shown in fig. 2, the radiative heat sources of CO and CH₄ close to the walls were obviously larger than those in the middle. The reason was that the temperature of the grid close to the walls varied quickly. Meanwhile, the pressure effect of line broadening close to the walls was evidently higher since a larger radiative heat source was obtained here. For CH₄, the maximum pressure effect of line broadening obtained by the LBL and SNB methods at pressures of 5, 10, and 30 atmosphere were less than 5% shown in figs. 2(a) and 2(b). While for the results of CO shown in fig. 2(c) and 2(d), neglecting the pressure effect of line broadening would dramatically under-predict the radiative heat sources using the LBL and SNB methods, especially for the radiative heat sources close to the walls. The maximum pressure effects of line broadening of CO were 55% and 65% calculated by the LBL and SNB methods, which were obviously larger than that of CH₄.

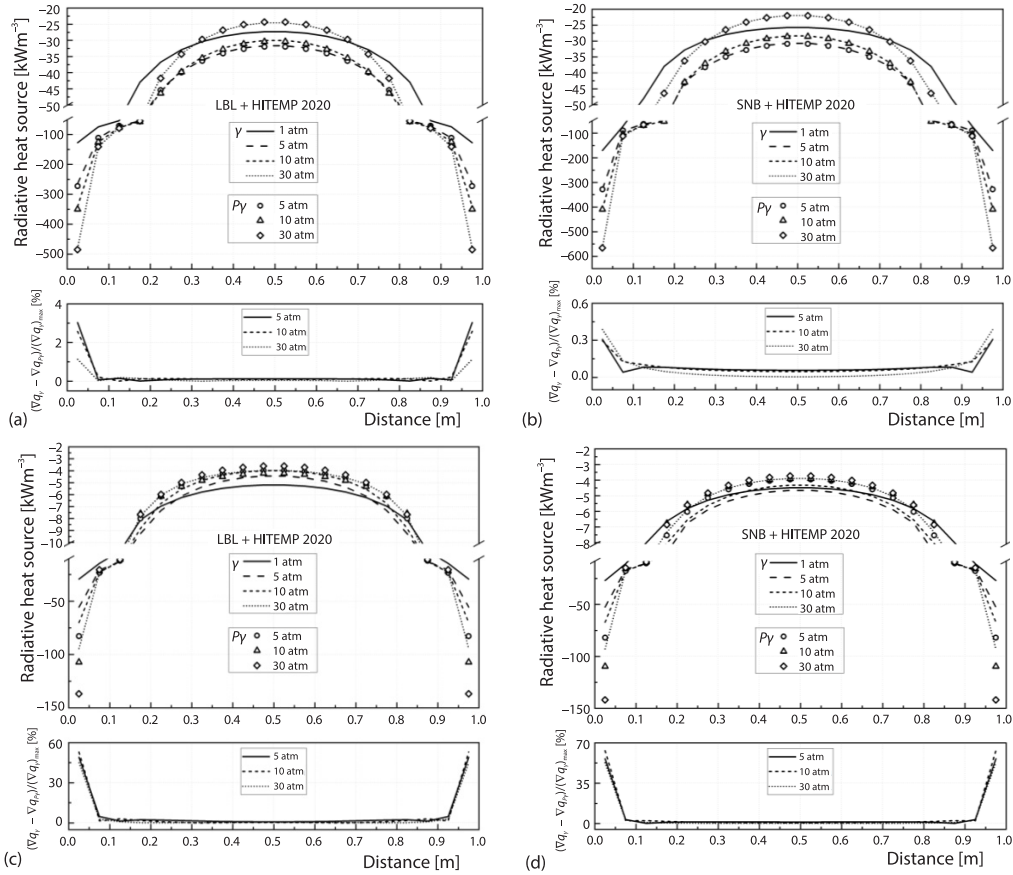


Figure 2. The pressure effect of line broadening on radiative heat source of;
(a) CH₄ calculated using LBL + HITEMP 2020, (b) CH₄ calculated using SNB +
HITEMP 2020, (c) CO calculated using LBL + HITEMP 2019, and
(d) CO calculated using SNB + HITEMP 2019 in Case 1

Radiative heat source for Case 2

In Case 2, an inhomogeneous and non-isothermal case was simulated which was conducted from [33]. The radiative heat sources calculated using parameters derived from eqs. (3) and (4) are compared in fig. 3. It is interesting to observe from fig. 3 that the maximum pressure effect of line broadening appeared at the position where the maximum radiative heat source occurred, which is the same as Case 1. It is clear from figs. 3(a) and 3(b) that little difference can be found between the radiative heat sources calculated by eqs. (3) and (4) for CH₄, whichever method was used. This result indicated that the pressure effect of line broadening had little impact on the radiative heat transfer of CH₄. As shown in fig. 3(c) and 3(d), the maximum pressure effects of line broadening of CO calculated by LBL and SNB methods were both over 30% at the pressure of 5 atmosphere. In addition, they increased with pressure and reached 50% at the pressure of 30 atmosphere. The results calculated by [33] using HITEMP 2010 database were also plotted in fig. 3(c) to study the effect of different databases on the radiative heat source. As shown in fig. 3(c), little difference could be found between the results of Brittes [33] and HITEMP 2019 database.

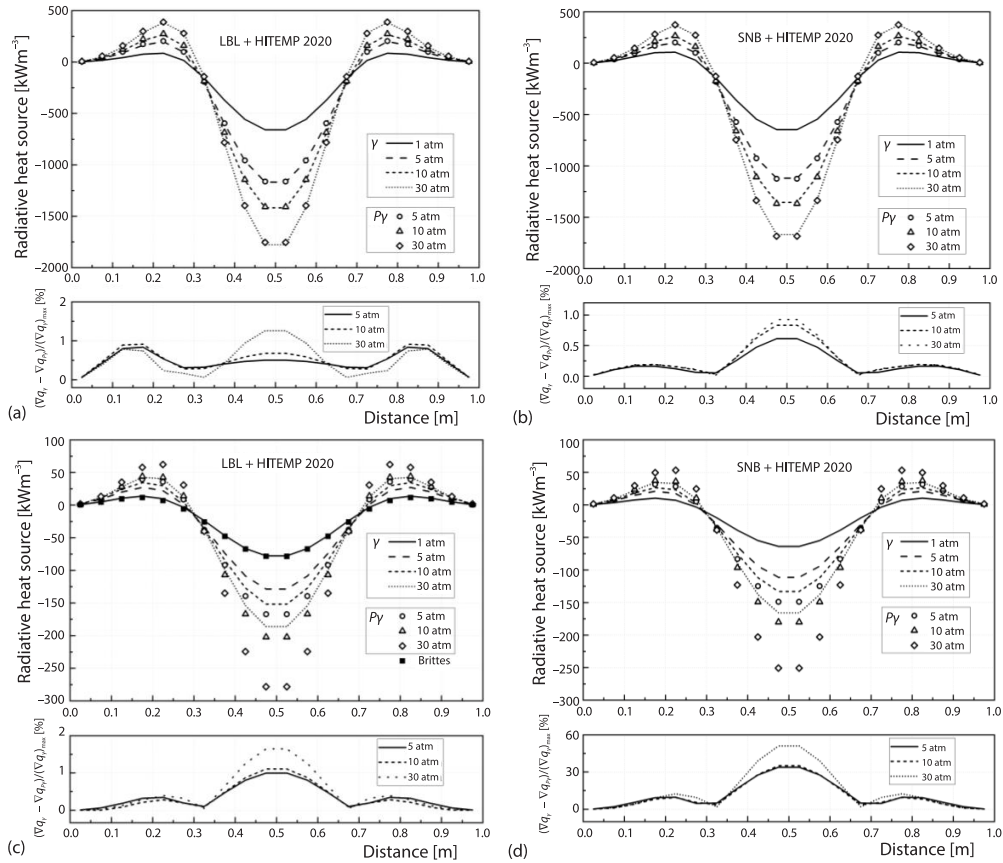


Figure 3. The pressure effect of line broadening on radiative heat source of; (a) CH₄ calculated using LBL + HITEMP 2020, (b) CH₄ calculated using SNB + HITEMP 2020, (c) CO calculated using LBL + HITEMP 2019, and (d) CO calculated using SNB + HITEMP 2019 in Case 2

Planck mean absorption coefficient

The Planck mean absorption coefficients, K_p , of CH₄ calculated with HITEMP 2020 database were shown in fig. 4. Please note, since the K_p calculated at 1, 5, 10, and 30 atmosphere using eq. (3) were the same, only the K_p calculated using eq. (3) at 1 atmosphere were plotted in fig. 4. The legends $P\gamma$ in fig. 4 represented the results calculated using eq. (4). The pressure effect of line broadening for the Plank mean absorption coefficient was described:

$$\frac{|K_{p,1atm} - K_{p,P\gamma}|}{(K_{p,1atm})_{max}} \quad (14)$$

The K_p calculated by [34] using the LBL method with high resolution transmission (HITRAN) 2008 database at 1 atmosphere were also potted in fig. 4 to investigate the effect of different databases on K_p .

As shown in fig. 4(a), the K_p calculated with HITEMP 2020 database is apparently larger than that with HITRAN 2008 database at 1 atmosphere above 600 K due to the lack of hot lines in HITRAN 2008 database. Hence, when the K_p of CH₄ is needed in the practical

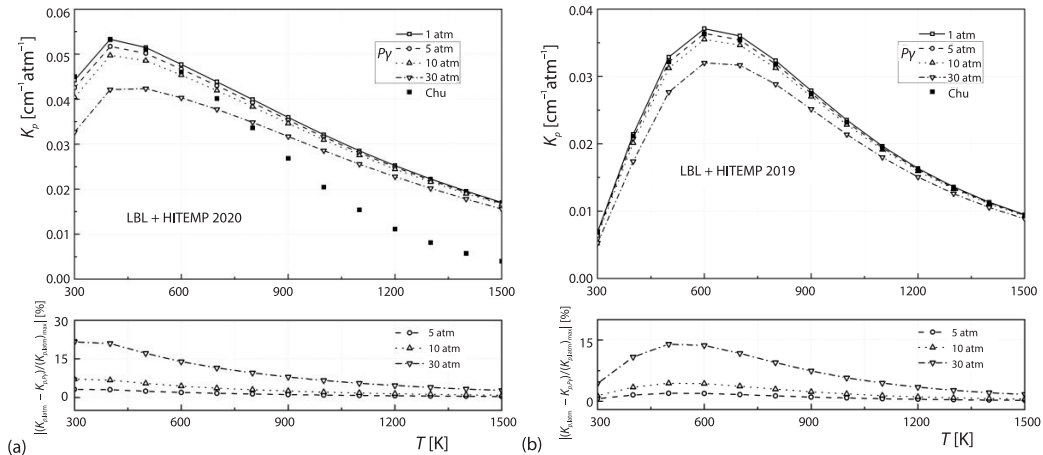


Figure 4. The pressure effect of line broadening on the Planck mean absorption coefficients of; (a) CH_4 and (b) CO calculated using HITEMP 2020 and HITEMP 2019 databases

prediction at a temperature above 600 K, the HITEMP 2020 database is more suggested. When considering the pressure effect of line broadening at elevated pressures, the K_p were obviously lower than that at 1 atmosphere and decreased as the pressure increased. As the pressure increased from 5 atmosphere to 30 atmosphere, the maximum pressure effect of line broadening increased from 3-22%. The pressure effect of line broadening at elevated pressures decreased as the temperature increased from 300-1500 K.

The K_p of CO calculated with HITEMP 2019 database were plotted in fig. 4(b). The results of Chu *et al.* [34] calculated with HITEMP 2010 database were also plotted in the fig. 4(b). In fig. 4(b), the K_p calculated with HITEMP 2020 database were a little larger than that with Chu *et al.* [34], especially at the temperature range of 500-700 K. The reason was that more hot lines existed in HITEMP 2020 database compared with HITEMP 2010 database. As shown in fig. 4(b), with temperature increased, the pressure effect of line broadening increased initially then decreased at three different pressures. It is clear from fig. 4(b) that without considering the pressure effect of line broadening would overpredict the K_p . The maximum pressure effects of line broadening obtained at 5 and 10 atmosphere were under 5%, which were obviously lower than that at a pressure of 30 atmosphere (14%). Though the pressure effect of line broadening of CO calculated at pressures of 5, 10, and 30 atmosphere were less than 20%, a larger error would appear when higher pressure was used.

Conclusions

A 1-D enclosure filled with isothermal homogeneous or non-isothermal inhomogeneous CO/CH_4 medium was simulated to investigate the pressure effect of line broadening on the radiative heat transfer. The radiative heat sources and Planck mean absorption coefficient at elevated pressures were calculated using LBL and SNB methods with lasted HITEMP databases. The conclusions of this study are as follows.

- For the CH_4 medium, the pressure effect of line broadening on radiative heat transfer can be neglected when HITEMP 2020 database was used, especially when the SNB method was adopted compared with the LBL method.
- For CO medium, the pressure effect of line broadening was obviously higher than that of CH_4 medium. The maximum pressure effect of line broadening was over 40% for non-iso-

thermal inhomogeneous case, and over 60% for isothermal homogeneous case at a pressure of 30 atmosphere.

- Without considering the pressure effect of line broadening would overpredict the K_p of CO and CH₄ media. The pressure effect of line broadening on K_p increased with pressure. The pressure broadening has a strong effect on the Planck mean absorption below 1000 K for CH₄ and at the temperature of 500-900 K for CO at 30 atmosphere. The maximum pressure effects of line broadening were 22% and 18% for CH₄ and CO at 30 atmosphere.
- When the temperature was above 600 K, the HITEMP 2020 database was suggested to calculate the K_p of CH₄. The K_p of CO calculated with HITEMP 2019 database were a little larger than that with HITEMP 2010 database.

Acknowledgment

This research was supported by the National Key Research Development Program of China (No.2017YFB0601900), the National Natural Science Foundation of China (No. 51976057, 51922040 and 51776078), the Foundation of State Key Laboratory of Coal Combustion (No. FSKLCCA2104), the Hunan Science and Technology Planning Project (2020RC5008) and the Fundamental Research Funds for the Central Universities (No. 2020JG005, 2020DF01).

Nomenclature

F – Lorentz line shape profile, [cm]
 f – mole fraction of the radiating gas, [-]
 I_b – spectral blackbody intensity, [Wm⁻²]
 K_p – Planck mean absorption coefficient, [cm⁻¹atm⁻¹]
 k – absorption coefficient of narrow band, [cm⁻¹]
 L – distance between two plates, [m]
 N – molecule density of the radiating gas, [cm⁻³]
 n – coefficient of temperature dependence, [-]
 P – pressure, [atm]
 q – radiative heat flux, [Wm⁻²]
 S – line intensity, [cm]
 T – temperature, [K]

Greek symbols

γ – half-width at half-maximum, [cm⁻¹]
 γ_{air} – air-broadened half-width, [cm⁻¹atm⁻¹]
 γ_{self} – self-broadened half-width, [cm⁻¹atm⁻¹]
 δ – average interval between spectral lines, [cm⁻¹atm⁻¹]
 ε – emissivity, [-]
 κ – spectral absorption coefficient, [cm⁻¹]

μ – cosine of the angle between radiative heat flux and intensity directions, [-]
 τ – transmissivity, [-]
 Ω – solid angle, [sr]
 ω – weight of radiative intensity in DOM method, [-]

Subscript

s – partial pressure
 sv – wave number
 w – boundary walls
 0 – reference state

Acronyms

ALBDF – absorption-line blackbody distribution function
DOM – discrete ordinate method
HITEMP – high temperature molecular spectroscopic
HITRAN – high resolution transmission
LBL – line-by-line
RTE – radiative transfer equation
SNB – statistical narrow band

References

- [1] Hamins, A., et al., Heat Feed back to the Fuel Surface, *Combustion Science and Technology*, 97 (1994), 1-3, pp. 37-62
- [2] Alberti, M., et al., Absorption of Infrared Radiation by Carbon Monoxide at Elevated Temperatures and Pressures – Part A: Advancing the Line-by-Line Procedure Based on HITEMP-2010, *Journal of Quantitative Spectroscopy and Radiative Transfer*, 200 (2017), Oct., pp. 258-271
- [3] Xie, Y., et al., Experimental and Numerical Study on Laminar Flame Characteristics of Methane Oxy-Fuel Mixtures Highly Diluted with CO₂, *Energy & Fuels*, 27 (2013), 10, pp. 6231-6237

- [4] Han, M., et al., Laminar Flame Speeds of H₂/CO with CO₂ Dilution at Normal and Elevated Pressures and Temperatures, *Fuel*, 148 (2015), May, pp. 32-38
- [5] Hargreaves, R. J., et al., An Accurate, Extensive, and Practical Line List of Methane for the HITEMP Database, *The Astrophysical Journal Supplement Series*, 247 (2020), 2, pp. 55-73
- [6] Consalvi, J. L., Liu, F., Radiative Heat Transfer in the Core of Axisymmetric Pool Fires – I: Evaluation of Approximate Radiative Property Models, *International Journal of Thermal Sciences*, 84 (2014), Oct., pp. 104-117
- [7] Venugopal, D., et al., Air and Oxygen Gasification Simulation Analysis of Sawdust, *Thermal Science*, 23 (2019), 2B, pp. 1043-1053
- [8] Escudero, M., et al., Analysis of the Behaviour of Biofuel-Fired Gas Turbine Power Plants, *Thermal Science*, 16 (2012), 3, pp. 849-864
- [9] Jakobs, T., et al., Gasification of High Viscous Slurry R&D on Atomization and Numerical Simulation, *Applied Energy*, 93 (2012), May, pp. 449-456
- [10] Ren, T., et al., Monte Carlo Simulation for Radiative Transfer in a High-Pressure Industrial Gas Turbine Combustion Chamber, *Journal of Engineering for Gas Turbines and Power*, 140 (2018), 5, 051503
- [11] Ilić, M. N., et al., Numerical Simulation of Wall Temperature on Gas Pipe-Line Due to Radiation of Natural Gas during Combustion, *Thermal Science*, 16 (2012), Suppl. 2, pp. S567-S576
- [12] Coelho, F. R., Franca, F. H., The WSGG Correlations Based on HITEMP2010 for Gas Mixtures of H₂O and CO₂ in High Total Pressure Conditions, *International Journal of Heat and Mass Transfer*, 127 (2018), Dec., pp. 105-114
- [13] Pearson, J. T., et al., Effect of Total Pressure on the Absorption-Line Blackbody Distribution Function and Radiative Transfer in H₂O, CO₂, and CO, *Journal of Quantitative Spectroscopy and Radiative Transfer*, 143 (2014), Aug., pp. 100-110
- [14] Chu, H., et al., Effects of Total Pressure on Non-Grey Gas Radiation Transfer in Oxy-Fuel Combustion Using the LBL, SNB, SNBCK, WSGG, and FSCK methods, *Journal of Quantitative Spectroscopy and Radiative Transfer*, 172 (2016), Mar., pp. 24-35
- [15] Zhou, Z., et al., Numerical Investigation on Effects of High Initial Temperatures and Pressures on Flame Behavior of CO/H₂/Air Mixtures Near the Dilution Limit, *International Journal of Hydrogen Energy*, 38 (2013), 1, pp. 274-281
- [16] Modest, M. F., *Radiative Heat Transfer*, Academic Press, New York, USA, 2013
- [17] Tien, C. L., Thermal Radiation Properties of Gases, *Advances in Heat Transfer*, 5 (1969), pp. 253-324
- [18] Ranganathan, S. K., et al., Numerical Model and Experimental Validation of the Heat Transfer in Air Cooled Solar Photovoltaic Panel, *Thermal Science*, 20 (2016), Suppl. 4, pp. S1071-S1081
- [19] Lakshmisha, K. N., et al., On the Flammability Limit and Heat Loss in Flames with Detailed Chemistry, *Symposium (International) on Combustion*, 23 (1991), 1, pp. 433-440
- [20] Qiao, L., et al., A Study of the Effects of Diluents on Near-Limit H₂-Air Flames in Microgravity at Normal and Reduced Pressures, *Combustion and Flame*, 151 (2007), 1-2, pp. 196-208
- [21] Hofgren, H., Sundén, B., Evaluation of Planck Mean Coefficients for Particle Radiative Properties in Combustion Environments, *Heat and Mass Transfer*, 51 (2015), 4, pp. 507-519
- [22] Zhou, Z., et al., Numerical Investigation on Effects of High Initial Temperatures and Pressures on Flame Behavior of CO/H₂/Air Mixtures Near the Dilution Limit, *International Journal of Hydrogen Energy*, 38 (2013), 1, pp. 274-281
- [23] Kuntz, M., Ho, M., Efficient Line-by-Line Calculation of Absorption Coefficients, *Journal of Quantitative Spectroscopy & Radiative Transfer*, 63 (1999), Sept., pp. 97-114
- [24] Sparks, L., Efficient Line-by-Line Calculation of Absorption Coefficients to High Numerical Accuracy, *Journal of Quantitative Spectroscopy and Radiative Transfer*, 57 (1997), 5, pp. 631-650
- [25] Kim, T. K., et al., Non-Gray Radiative Gas Analyses Using the S-N Discrete Ordinates Method, *Journal of Heat Transfer*, 113 (1991), 4, pp. 946-952
- [26] Malkmus, W., Random Lorentz Band Model with Exponential-Tailed \hat{S}^{-1} Line-Intensity Distribution Function, *Journal of the Optical Society of America*, 57 (1967), 3, 323
- [27] Chu, H., et al., A Comparison of Two Statistical Narrow band Models for Non-Gray Gas Radiation in Planar Plates, *Thermal Science*, 22 (2018), Suppl. 2, pp. S777-S784
- [28] Zheng, S., et al., The Effect of Different HITRAN Databases on the Accuracy of the SNB and SNBCK Calculations, *International Journal of Heat and Mass Transfer*, 129 (2019), Oct., pp. 1232-1241
- [29] Godson, W., The Evaluation of Infrared Radiative Fluxes Due to Atmospheric Water Vapour, *Quarterly Journal of the Royal Meteorological Society*, 79 (1953), 341, pp. 367-379

- [30] Soufiani, A., Taine, J., Application of Statistical Narrow-Band Model to Coupled Radiation and Convection at High Temperature, *International Journal of Heat and Mass Transfer*, 30 (1987), 3, pp. 437-447
- [31] Soufiani, A., Djavdan, E., A Comparison between Weighted sum of Gray Gases and Statistical Narrow-Band Radiation Models for Combustion Applications, *Combustion and Flame*, 97 (1994), 2, pp. 240-250
- [32] Chu, H., *et al.*, Calculations of Gas Thermal Radiation Transfer in 1-D Planar Enclosure Using LBL and SNB Models, *International Journal of Heat and Mass Transfer*, 54 (2011), 21-22, pp. 4736-4745
- [33] Brittes, R., *et al.*, ThenWSGG Model Correlations to Compute Non-Gray Radiation from Carbon Monoxide in Combustion Applications, *Journal of Heat Transfer*, 139 (2017), 4, 041202
- [34] Chu, H., *et al.*, Calculations of Narrow-Band Transmissivities and the Planck Mean Absorption Coefficients of Real Gases Using Line-by-Line and Statistical Narrow-Band Models, *Frontiers in Energy*, 8 (2014), 1, pp. 41-48